JOURNAL OF AIRCRAFT
Vol. 32, No. 5, September–October 1995

Engineering Notes

ENGINEERING NOTES are short manuscripts describing new developments or important results of a preliminary nature. These Notes cannot exceed 6 manuscript pages and 3 figures; a page of text may be substituted for a figure and vice versa. After informal review by the editors, they may be published within a few months of the date of receipt. Style requirements are the same as for regular contributions (see inside back cover).

Asymptotic Expression of the Forces Induced by a Strong Jet in a Crossflow

A. Dyment* and J. P. Flodrops†
ONERA–IMFL, 59000 Lille, France

Nomenclature

c = velocity of sound
d = diameter of the jet orifice
L = lift of the body
l = characteristic dimension of the body
M = Mach number
p = pressure
U = magnitude of the velocity vector
α = angle of attack
β = angle between Ox and the jet axis at exit
γ = ratio of specific heats
ρ = density

Subscripts
i = stagnation conditions
j = values in the jet at the exit of the nozzle
0 = no-jet conditions
∞ = values in the freestream

Introduction

THE phenomena relating the expansion of a lateral jet into a stream are too complex to be totally determined by means of pure theory, and so one has to resort to experimentation.

However, the prevision of full-scale global effects from wind-tunnel measurements on models is not completely satisfactory, especially in the case of hot jets. This is so because the dimensionless parameters, which evolve from a simple dimensional analysis, are numerous and because their invariance is, for some of them, difficult to satisfy.

Often the use of asymptotic analysis can improve the situation and give way to a better physical similarity.

Statement of the Problem

Consider a flow of air past a projectile that is characterized by its shape and length l (Fig. 1).

A jet emerges from an orifice of diameter d, which is very small compared to the projectile size. The jet is strong, either sonic or supersonic, so that the exit conditions are independent of the incoming flow. Ox is parallel to the freestream velocity and Oz is normal to Ox in the plane containing both the axis of the body and the jet exit. No side-slip is assumed, although this is not essential.

Received Nov. 14, 1994; revision received Jan. 22, 1995; accepted for publication Feb. 16, 1995.

*Head of the Fundamental Fluid Mechanics Group, 5 bd Painlevé.
†Senior Scientist, 5 bd Painlevé. Member AIAA.

Quantities such as the lift increase $\Delta L = L - L_0$ are of practical interest. Neglecting skin friction, ΔL can be expressed as

$$\Delta L = \int_S (p_0 - p) n \, dS - \gamma_j M_j^2 p_j \frac{\pi d^2}{4} \sin \beta \tag{1}$$

where S represents the projectile surface, including the nozzle orifice, and n is the z component of the outward directed normal.

Jet as a Point Source

Dimensional analysis indicates that ΔL is a function of β, γ, γ_j, M_∞, M_j, ρ_j/ρ_∞, U_j/U_∞, d/l, and α. As the orifice is very small, the jet can be regarded as a source of mass, momentum, and energy,[1] the rates of which are, respectively, proportional to $\rho_j U_j d^2$, $(p_j + \rho_j U_j^2) d^2$, and $(p_j/(\gamma_j - 1) + \rho_j U_j^2/2) d^2$, that is to $\gamma_j M_j \mathcal{Q}$, $(1 + \gamma_j M_j^2)(\mathcal{P}\mathcal{Q})^{1/2}$ and $[1/(\gamma_j - 1) + M_j^2/2]\gamma_j M_j \mathcal{P}$, with

$$\mathcal{Q} = (p_j/c_j) d^2, \qquad \mathcal{P} = p_j c_j d^2 \tag{2}$$

In this way, d is not a relevant parameter of its own, and the jet is characterized by only five parameters (β, γ_j, M_j, $\mathcal{P}$, $\mathcal{Q}$) in lieu of the initial six (β, γ_j, U_j, ρ_j, p_j, d).

Taking ρ_∞, U_∞, and l as primary quantities, the dimensionless parameters corresponding to $\mathcal{P}$ and $\mathcal{Q}$ can be obtained as $\rho_j U_j d^2/\rho_\infty U_\infty l^2$ and $(\rho_j U_j^3 d^2)/(\rho_\infty U_\infty^3 l^2)$. Either one of these two may be replaced by U_j/U_∞.

In the remainder, the parameter corresponding to $\mathcal{P}$ is kept because it will appear to be essential in some important asymptotic cases. Then, physical similarity leads to

$$\frac{\Delta L}{\rho_\infty U_\infty^2 l^2} = \text{function of} \left(\alpha, \beta, \gamma, \gamma_j, M_\infty, M_j, \frac{U_j}{U_\infty}, \frac{\rho_j U_j^3 d^2}{\rho_\infty U_\infty^3 l^2} \right) \tag{3}$$

Obviously, an equivalent form of (3) is

$$\frac{\Delta L}{\rho_\infty U_\infty^2 l^2} = \text{function of} \left(\alpha, \beta, \gamma, \gamma_j, M_\infty, M_j, \frac{c_j}{c_\infty}, \frac{c_j p_j d^2}{c_\infty p_\infty l^2} \right) \tag{4}$$

At first sight, the previous formal relations can be simplified, but extreme care must be exercised in doing so. The last quantity in (4) cannot be replaced by $(p_j d^2)/(p_\infty l^2)$ if c_j/c_∞ is not relevant to the problem, as we shall see in the following.

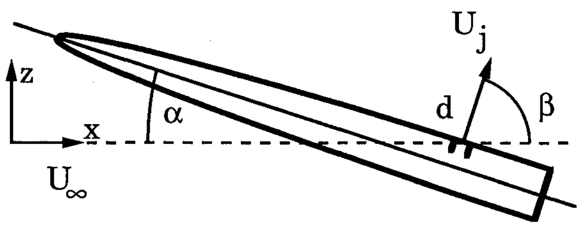

Fig. 1 Schematic drawing of the projectile.

Hot Jets and Highly Supersonic Jets

For hot jets, such as those created by the combustion of a powder charge, it is extremely difficult to satisfy the condition that c_j/c_∞ match in wind-tunnel tests and in the real case. It is known[2] that, asymptotically, for d decreasing to zero, a hot jet is equivalent to a source of energy, which means that it is represented by $\mathcal{P}$ only. As a consequence, c_j/c_∞ has no influence any more (in practice, this holds as soon as c_j/c_∞ is larger than 2).

Taking this result into account, (4) becomes

$$\frac{\Delta L}{\rho_\infty U_\infty^2 l^2} = \text{function of}\left(\alpha,\ \beta,\ \gamma,\ \gamma_j,\ M_\infty,\ M_j,\ \frac{c_j p_j d^2}{c_\infty p_\infty l^2}\right) \tag{5}$$

Another interesting case is to be found when the jet Mach number M_j is very large. Then, the three source rates become approximatively $\rho_j U_j d^2$, $\rho_j U_j^2 d^2$ and $(\rho_j U_j^3 d^2)/2$, i.e., $A = \gamma_j M_j \mathcal{Q}$, $(AB)^{1/2}$ and $B = \gamma_j M_j^3 \mathcal{P}$. M_j and γ_j have no effect of their own. Similarity yields

$$\frac{\Delta L}{\rho_\infty U_\infty^2 l^2} = \text{function of}\left(\alpha,\ \beta,\ \gamma,\ M_\infty,\ \frac{U_j}{U_\infty},\ \frac{\rho_j U_j^3 d^2}{\rho_\infty U_\infty^3 l^2}\right)$$

When d decreases to zero, the only physically admissible possibility is that U_j behaves as $d^{-2/3}$. Then A goes to zero and B remains finite, and so the parameter U_j/U_∞ disappears:

$$\frac{\Delta L}{\rho_\infty U_\infty^2 l^2} = \text{function of}\left(\alpha,\ \beta,\ \gamma,\ M_\infty,\ \frac{\rho_j U_j^3 d^2}{\rho_\infty U_\infty^3 l^2}\right) \tag{6}$$

Thus, a highly supersonic jet is also equivalent to a source of energy. But, whereas in the case of hot jets, internal and kinetic energies are of the same order of magnitude (as $M_j \sim 1$), here the latter is dominant.

Quasiexplicit Expressions

When the dimensionless parameter that contains d is very small, alternate function relations can be used. Accordingly, from (4)

$$\frac{\Delta L}{\rho_\infty U_\infty^2 l^2} = \left(\frac{p_j d^2}{p_\infty l^2}\right)^n \cdot \text{function of}\left(\alpha,\ \beta,\ \gamma,\ \gamma_j,\ M_j,\ \frac{c_j}{c_\infty}\right) \tag{7}$$

The exponent n can be experimentally determined by varying only one of the quantities p_j, p_∞, l, or d.

For hot jets and highly supersonic jets, (5) and (6), respectively, become

$$\frac{\Delta L}{\rho_\infty U_\infty^2 l^2} = \left(\frac{c_j p_j d^2}{c_\infty p_\infty l^2}\right)^n \cdot \text{function of}\ (\alpha,\ \beta,\ \gamma,\ \gamma_j,\ M_\infty,\ M_j)$$

$$\frac{\Delta L}{\rho_\infty U_\infty^2 l^2} = \left(\frac{\rho_j U_j^3 d^2}{\rho_\infty U_\infty^3 l^2}\right)^n \cdot \text{function of}\ (\alpha,\ \beta,\ \gamma,\ M_\infty)$$

Jet Emerging from a Plane Wall

Consider a simplified case where the projectile is replaced by an infinite wall, parallel to the freestream velocity. This special body has no characteristic length and L_0 is zero. It follows that l must disappear from the list of quantities relevant to the problem. As a consequence, the exponent n in (7) must be equal to 1:

$$\frac{\Delta L}{\rho_\infty U_\infty^2 d^2} = \left(\frac{p_j}{p_\infty}\right) \cdot \text{function of}\left(\beta,\ \gamma,\ \gamma_j,\ M_\infty,\ M_j,\ \frac{c_j}{c_\infty}\right) \tag{8}$$

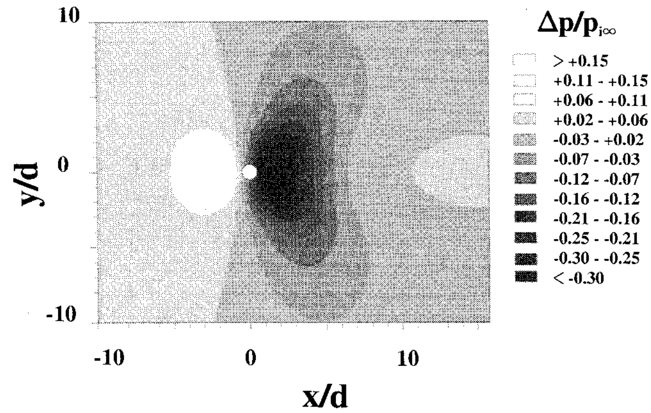

Fig. 2 Flat plate wall pressure increase $M_\infty = 0.8$, $M_j = 2$, and $p_{ij}/p_{i\infty} = 15.1$.

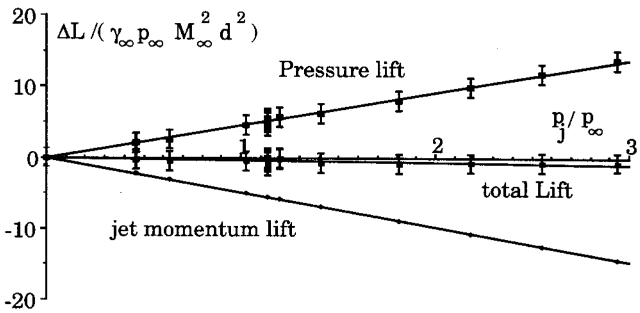

Fig. 3 Flat plate lift increase $M_\infty = 0.8$ and $M_j = 2$.

In the course of experiments about the unsteady properties of such lateral jets, some steady-state measurements have been performed at ONERA–IMFL. A small supersonic nozzle, of exit diameter $d = 5$ mm, was mounted in the flat bottom wall of a transonic wind tunnel, with its axis perpendicular to the wall. Air was used for the jet and experimental conditions were kept constant at $\beta = 90$ deg, $\gamma = \gamma_j = 1.4$, $M_\infty = 0.8$, $p_{i\infty} = 10^5$ Pa, $c_{i\infty} = c_{ij} = 340$ m/s, and $M_j = 2$, except for the jet stagnation pressure p_{ij}, which ranged between 2.3–15.1 times $p_{i\infty}$. Wall pressure was obtained from some 60 pressure taps that were distributed on the tunnel wall, mainly on one side of the tunnel axis, although some were used to check symmetry of the flow. From successive readings, the uncertainty on the pressure measurements can be estimated at about $\pm\frac{1}{2}$ mm of mercury.

In Fig. 2 an example of the modification of the pressure field on the wall caused by the existence of the jet for the highest stagnation pressure ratio is shown.

The values of the terms of the right side of relation (1) were computed and are shown in Fig. 3 for different values of $p_{ij}/p_{i\infty}$. As the pressure taps were not regularly distributed on the wall, the computation of the pressure term required some interpolation before numerical integration. The indicated uncertainty on the lift increase was computed assuming a change of twice the pressure measurement uncertainty for each tap in the same direction. The jet momentum was directly computed from the measured jet stagnation pressure and, as the other flow parameters are kept constant, it obviously is proportional to p_j. It can also be noticed from Fig. 3 that, within the experimental uncertainty, the lift increase due to the wall pressure changes is proportional to p_j, which is consistent with formula (8). The resultant lift is very small since the jet impulse is balanced by the global effect of the pressure field induced by the jet.

This result gives some evidence of the relevance of the asymptotic approach.

References

[1]Dyment, A., and Merlen, A., "Gun Firing Similarity for Aircraft Interference Problems," *Journal of Aircraft*, Vol. 18, No. 5, 1981, pp. 415, 416.

[2]Merlen, A., and Dyment, A., "Similarity and Asymptotic Analysis for Gun Firing Aerodynamics," *Journal of Fluid Mechanics*, Vol. 225, pp. 497–528.

Viscous Flow Past a Nacelle in Proximity to a Flat Plate

Kamran Fouladi*

Lockheed Engineering and Sciences Company, Inc., Hampton, Virginia 23666

Introduction

VARIOUS conceptual designs for a commercial supersonic transport have been developed in recent years. Most of these configurations have been designed using linearized and modified linearized potential theory methodologies[1–5] to define the vehicle shape and the aerodynamic characteristics. Other methods based on Whitham's modified linear theory[6–8] have been used in the design and analysis of low-boom configurations. The combination of these methods has proven to be useful in the preliminary design stage of low-boom, high-speed civil transport configurations.

In estimating the overall aerodynamic characteristics of a configuration with nacelles, the interference effects must be evaluated. The lift induced by nacelles on the wing lower surface adds to the equivalent body area distributions composed of volume and lift contributions. The equivalent body area rule defines Whitham's F-function, which in turn renders the far-field overpressure signatures of a supersonic aircraft. The computational technique described in Ref. 4 provides estimations of the loads imposed on a wing surface by nacelles mounted nearby. This numerical method, however, is impaired by its inability to account for certain nonlinear effects inherent in complicated flows. The qualitative analyses of wind-tunnel data for various aircraft models with nacelles have suggested that the interference pressures, calculated using the computer program of Ref. 4, might be underestimated in the extreme near field. Therefore, more accurate estimates of the extreme near-field conditions are required to improve the design of low-boom supersonic transport configurations.

The purpose of the present study is to perform Navier–Stokes calculations in order to provide pressure distributions and force data on a flat plate with a nacelle in close proximity. The pressure distributions obtained using Navier–Stokes equations are then compared with the pressure distributions obtained using the linear theory of Ref. 4. Incorporating the nacelle-induced lift on the wing into the design process of a low-boom transport configuration will be included in a follow-up study. The Navier–Stokes equations are solved by an implicit, approximately factored, finite volume, upwind algorithm.[9,10] Baysal et al.[9] have used this algorithm to compute a supersonic flow past an ogive-nose-cylinder at zero-deg angle of attack near a flat plate on a composite mesh of overlapped grids. Fouladi et al.[10–11] extended the algorithm to include the use of a hybrid domain decomposition method that takes advantage of strengths of various techniques such as multiblock structured grids, zonal grids, or overlapped grids. This Note presents the numerical investigations of viscous supersonic flows past a circular nacelle placed in close proximity to a flat plate. The interference flowfield between these two geometrically nonsimilar components is simulated for several freestream Mach numbers.

Received Dec. 12, 1994; revision received June 12, 1994; accepted for publication Feb. 22, 1995.

*Engineer, Aeronautics and Management Support Department, Langley Program Office.

Results and Discussion

In the present investigation, a circular nacelle is placed in close proximity to a flat plate. The nacelle is 36 ft long and its schematic is detailed in Fig 1. Inlet and exhaust diameters of the nacelle are 6.0 and 9 ft, respectively. The flat plate is 41.86 ft long and 14.44 ft wide, and it is located 5.5 ft from the nacelle centerline. The longitudinal center planes of the nacelle and the flat plate are aligned. Two multiblock-structured Cartesian grids represent the upper (105 × 29 × 25) and lower (105 × 29 × 37) sides of the flat plate, and they are both overlapped on the outer H—O grid (105 × 33 × 45) of the nacelle. The inner H—O grid (93 × 33 × 33) of the nacelle is matched with the outer grid of the nacelle along the nacelle wall. The total number of grid points for this composite grid is 445,992. Only half of the configuration is analyzed because the model is symmetric and at zero yaw angle. The computational time and run-time memory for the present computations on the Cray-2 at the NASA Langley Research Center are approximately 6 CPU hours and 17 MWords, respectively.

The boundary conditions are specified explicitly in this implicit scheme. The conventional viscous boundary conditions are imposed on all solid surfaces. The upstream boundaries are all specified. First-order extrapolations of the primitive variables are used along the downstream boundary. One-dimensional characteristic boundary conditions are imposed at the outer boundary of the nacelle and at top and spanwise outboard boundaries of the flat plate. Reflection boundary conditions are used on the plane of symmetry. Intergrid boundaries also exist between overlapped subdomains that do not coincide with the physical boundaries of the computational domain. The boundary conditions for the intergrid boundaries are given in detail in Ref. 9. Three different freestream Mach numbers M_∞ of 1.6, 2.0, and 2.3 are considered.

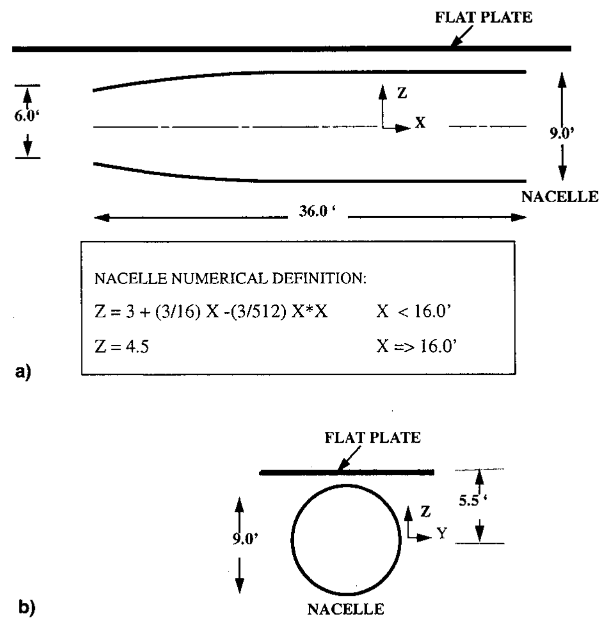

Fig. 1 Schematic of the nacelle in proximity to the flat plate: a) side and b) back view.